Supplementary material for

How secure are the adversarial examples themselves?

[1]Hui Zeng, [1]Kang Deng, [2]Biwei Chen, and [1]Anjie Peng

[1]School of Computer Science and Technology, Southwest University of Science and Technology, 621010, China
[2]Center for Data Science Analysis, Houghton College, NY 14744, USA
penganjie200012@163.com

Due to the page limitation of our submission to ICASSP2022, we provide more details about experiments in this document.

Experiment Settings

Our experiments are conducted on a subset of the ImageNet validation dataset. This subset is composed of 6000 images, which belong to 1000 classes. We split these 6000 images into two halves. The first 3000 images are used for training an ensemble classifier and for obtaining the relationship of σ and P_{fa}^{1} in $\delta^{1}()$, and the relationship of *t* and P_{fa}^{2} in $\delta^{2}()$.Taking the BIM attack for example, we add Gaussian noise $N(0,\sigma^2)$ to 3000 benign images and then denoise them with the same parameter σ. P_{fa}^{1} is calculated as the probability that the classification result has been changed after noise addition-then-denoising. The relationship between σ and P_{fa}^{1}can be obtained by varying σ. Similarly, we use 2000 (benign, adversarial) image pairs to train an ensemble classifier and use the trained classifier to classify the remaining 1000 benign images. Here the adversarial images are generated with mixed attack strengths, and the number of sub-classifiers is set as *N*=51. By doing so, the relationship between *t* and P_{fa}^{2} can be obtained.[1]

The remaining 3000 images are used for testing. A successful attack is declared when $F(\boldsymbol{I}') = y_t$. To make the attack more practical, $\boldsymbol{I}'$ is saved in PNG format before checking its attacking efficiency. The two-step test is then performed only on the successfully attacked images. For the constrained perturbation attacks, $\epsilon \in \{1, 2, 4, 6, 8\}$. For the optimized perturbation attacks, $k \in \{0, 5, 10, 15, 20\}$. Preliminary experiments suggest that Nash equilibrium will not exist in the region of $\epsilon > 8$ or $k > 20$. The strategy of

[1] Some of previous works [1, 2] excluded the images that cannot be correctly predicted by the CNN classifier, i.e.,$F(\boldsymbol{I}) \neq y_{true}$, in calculating false alarm rate. In our experiments, we did not exclude such images based on the following considerations: 1. the spatial instability of the images that can be correctly classified and that cannot be correctly classified is statistically different. The former is usually stronger than the latter. 2. We focus on the targeted attack, which means all images can be used as a cover in attacking. Note in untargeted attacks, only images that are correctly classified can be used as a cover.

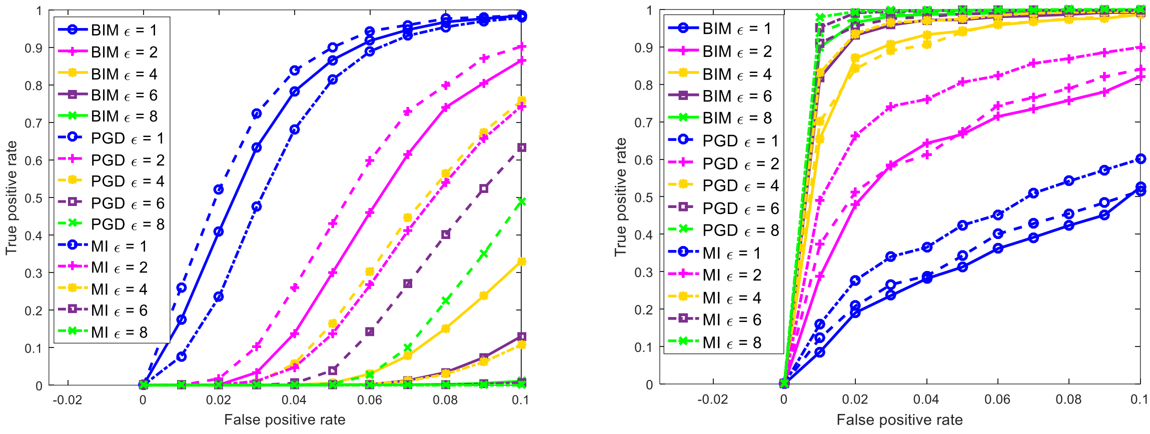

(a) (b)

Fig.1. ROC performance of the two single tests on perturbation-constrained attacks. (a) Noise addition-then-denoising test, (b) SRM based test.

the investigator is $P_{fa}^1 \in \{0: 0.01: P_{fa}\}$. Since the detection performance in the low P_{fa} area is more critical in practice, the upper bound of P_{fa} is set as 0.1.

Detection performance of each single test

To supplement Figure 4 of the paper, we show the ROC performance of the two single tests on three perturbation-constrained attacks in Fig. 1. The solid lines, dotted lines, and dot-dash lines denote ROC curves of BIM attack, PGD attack, and MI attack, respectively.

Adversarial example security

To supplement Figure 6 of the paper, we show the P_d matrices when $P_{fa} = 0.03$ and $P_{fa} = 0.04$ for various attacks in Fig. 2 and 3.

Numerical solution of the games

To make our work easier for readers, we introduce the numerical solution to the Adversarial-detection game as follows. Specifically, we take the BIM attack, P_{fa}=0.04 as an example (Fig. 3(a)). The P_d matrix is given below:

$$
\begin{array}{llllll}
P_d = [& \mathbf{0.2813} & \mathbf{0.3651} & 0.5344 & 0.6667 & 0.7840; \\
 & 0.6429 & 0.5855 & \mathbf{0.4806} & \mathbf{0.3131} & 0.1358; \\
 & 0.9330 & 0.9083 & 0.8695 & 0.6561 & \mathbf{0} \quad ; \\
 & 0.9718 & 0.9586 & 0.9312 & 0.8175 & \mathbf{0} \quad ; \\
 & 0.9868 & 0.9824 & 0.9656 & 0.8995 & \mathbf{0} \quad]
\end{array}
$$

We provide two ways to find its Nash equilibrium (NE).

The first one is using equation (9) of the paper, which assumes the investigator move first and allows the attacker to respond. According to (9), we first find the minimum element of each column.

min(P_d) = [0.2813 0.3651 0.4806 0.3131 0]

Then, the maximum value of min(P_d) is regarded as the payoff under NE.

max(min(P_d)) = 0.4806

The corresponding NE point is (P_{fa}^1 =0.02, $\epsilon = 2$).

The other way is to resort to mixed-strategy NE, which allows both players to move simultaneously. The mixed-strategy NE could be calculated with the Disciplined Convex Programming toolbox (available at: cvxr.com/cvx/). In our example, the calculated NE can be described as follows:

The attacker chooses $\epsilon = 1$ with the probability of 0.39 and chooses $\epsilon = 2$ with 0.61.

The investigator chooses $P_{fa}^1 = 0$ with the probability of 0.13 and chooses $P_{fa}^1 =$ 0.02 with 0.87.

The payoff under the mixed-strategy NE is 0.5016.

Fig. 4 shows the Nash equilibrium ROCs of both solution strategies for BIM attack. The NEROC obtained under Maxmin-strategy is similar to that under mixed-strategy NE. Hence, we adopt the Maxmin-strategy due to its comprehensibility in our study.

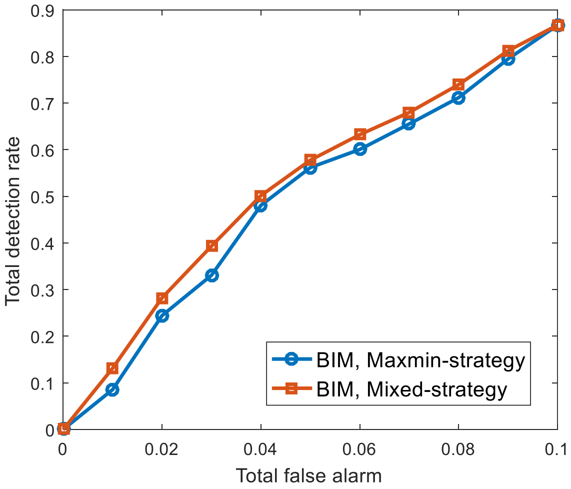

Fig.4. Nash equilibrium ROC of the adversarial-detection game when the attacker utilizing BIM attack.

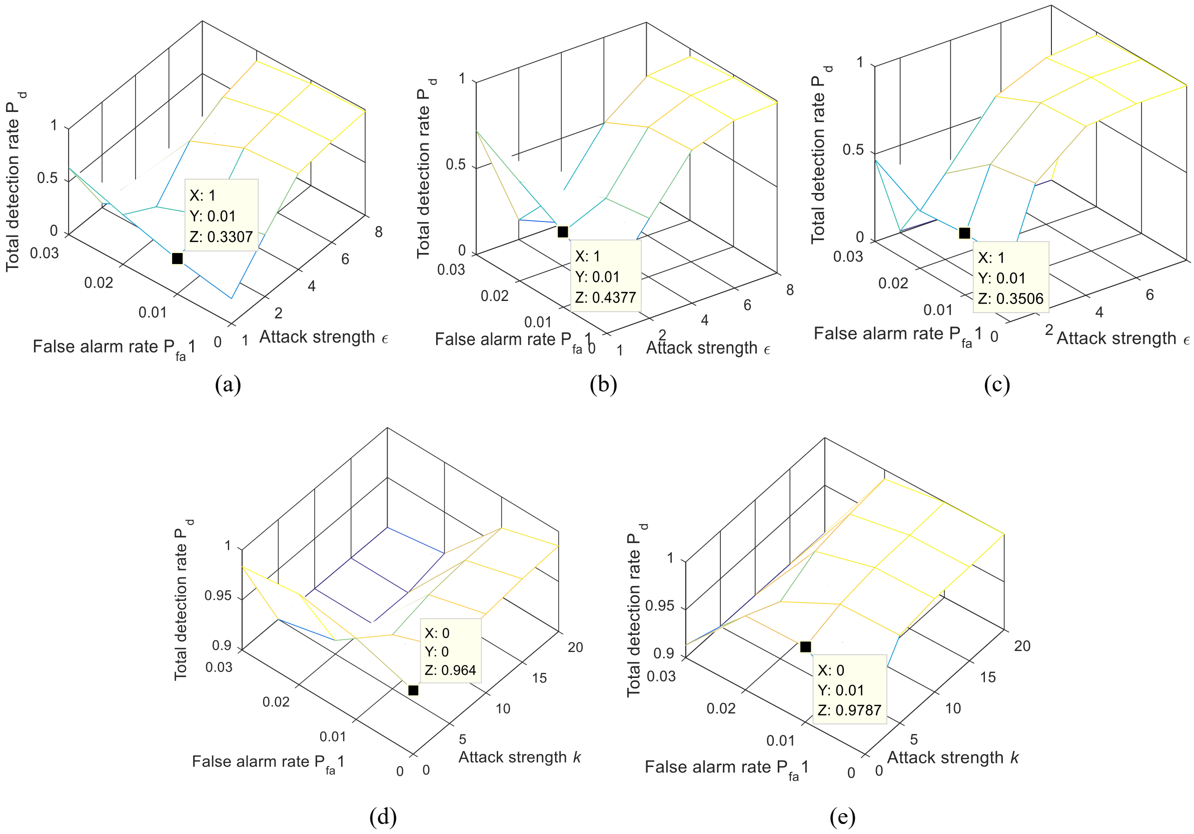

(a) (b) (c)

(d) (e)

Fig.2. P_d matrix and the corresponding NE when $P_{fa} = 0.03$. (a) BIM attack, (b) PGD attack, (c) MI attack, (d) C&W attack, (e) ST attack.

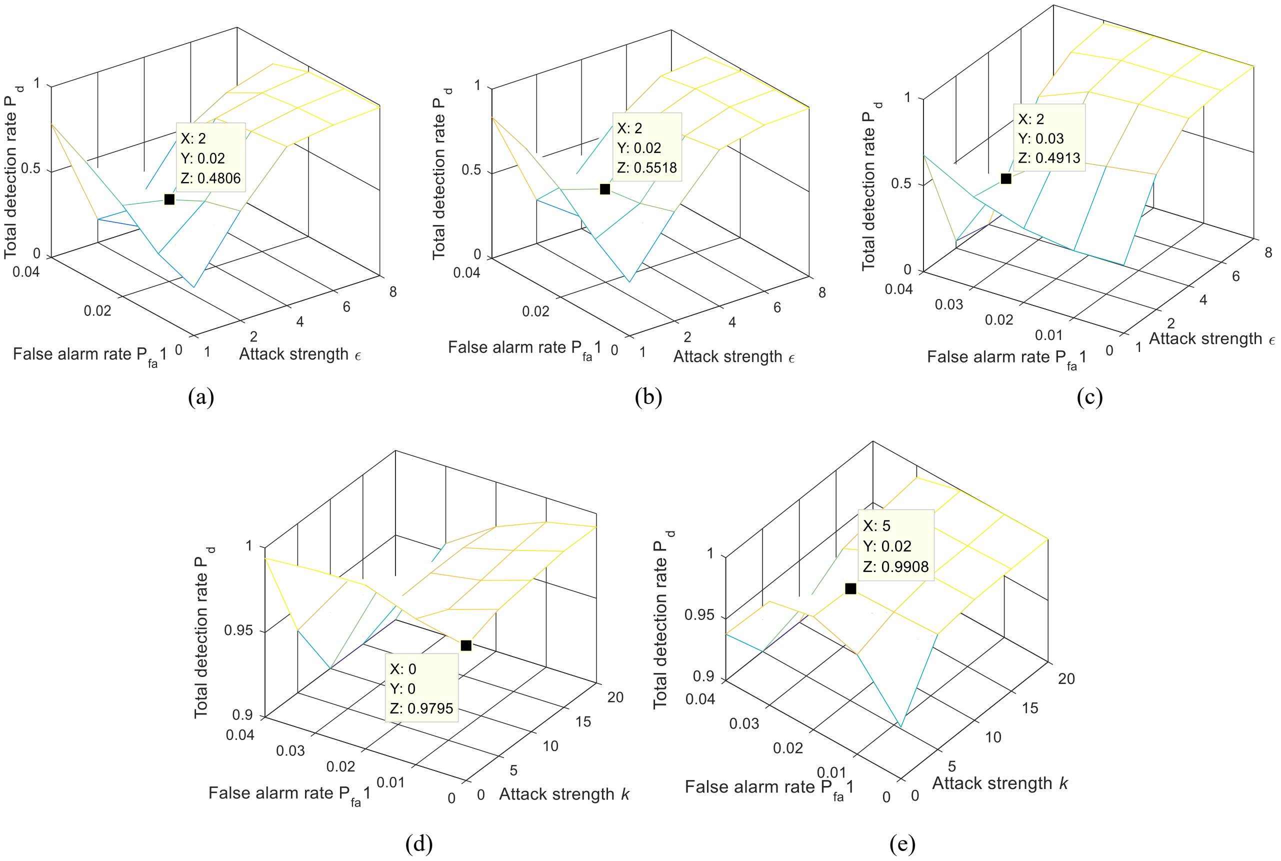

(a)

(b)

(c)

(d)

(e)

Fig.3. P_d matrix and the corresponding NE when $P_{fa} = 0.04$. (a) BIM attack, (b) PGD attack, (c) MI attack, (d) C&W attack, (e) ST attack.

References

1. B. Liang, H. Li, M. Su, et al., “Detecting adversarial image examples in deep neural networks with adaptive noise reduction,” IEEE Transactions on Dependable and Secure Computing, doi: 10.1109/TDSC.2018.2874243, 2018
2. K. Deng, A. Peng, H. Zeng, “Detecting C&W adversarial images based on noise addition-then-denoising,” To appear in International conference on image processing, 2021